Supplementary Information

Tuning Lattice and Porosities of 2D Imine Covalent Organic Frameworks by Chemically Integrating 4-Aminobenzaldehyde as Bifunctional Linker

Qing Sun, [1, 2] Hongyun Niu, [2] Yali Shi, [1, 2] Yongliang Yang, [2, 4] Yaqi Cai[1, 2, 3, 4, *]

[1]School of Environment, Hangzhou Institute for Advanced Study, University of Chinese Academy of Sciences, Hangzhou 310024, China

[2]State Key Laboratory of Environmental Chemistry and Ecotoxicology, Research Center for Eco-Environmental Sciences, Chinese Academy of Sciences, Beijing 100085, China

[3]Hubei Key Laboratory of Environmental and Health Effects of Persistent Toxic Substances, School of Environment and Health, Jianghan University, Wuhan 430056, China

[4]University of Chinese Academy of Sciences, Beijing 100049, China

[*]Correspondence: caiyaqi@rcees.ac.cn (Y. Cai).

Table of Contents

Section S1 General Information

1.1 Chemicals and reagents

All reagents were purchased from commercial sources and used without further purification.

1,3,5-triformylphloroglucinol (Tp), 1,3,5-Tris(4-aminophenyl)benzene (TAPB), 1,3,5-tris(4-aminophenyl)triazine (TAPT) were obtained from Jilin Chinese Academy of Sciences - Yanshen Technology Co., Ltd. (Jilin, China). 1,4-phenylenediamine (Pa-1), anhydrous 1,4-dioxane and mesitylene were purchased from J&K Scientific Ltd. (Beijing, China). 2,5-dimethyl-p-phenylenediamine (Pa-2), 4-aminobenzaldehyde (ABA) were acquired from Shanghai Aladdin Biochemical Technology Co., Ltd. (Shanghai, China).

1.2 Characterization

Powder X-ray diffraction (PXRD) data were collected from a Bruker D8-ADVANCE diffractometer (Bruker, Germany) using a Cu Kα (λ = 1.5418 Å) radiation ranging from 2º to 30º with a resolution of 0.02°.

Fourier transform infrared (FTIR) spectra in the 4000–400 cm^{-1} region was recorded on a Nicolet iS10 FTIR spectrometer (Thermo Fisher Scientific, Waltham, MA).

Solid-state nuclear magnetic resonance (ssNMR) spectra were obtained on a 600 MHz Bruker Avance III spectrometer (Bruker, Germany).

Surface analysis by X-ray photoelectron spectroscopy (XPS) was carried out using Thermo Fisher ESCALAB 250Xi equipment (Waltham, MA), and the X-ray source was Al Kα radiation (1486.6 eV, monochromatic).

Elemental analysis (EA) was conducted on an Vario EL cube elemental analyzer (Elementar, Germany).

Surface area and pore volume were measured by Brunauer-Emmett-Teller (BET) methods (ASAP2460; Micrometritics, Norcross, GA).

Thermogravimetric analysis (TGA) curves were recorded on a TGA/DSC 3+ thermal analysis system under N_2-flow (METTLER TOLEDO, Swiss).

Section S2 Synthetic Procedures

COF TpPa-1 and TpPa-2: Following a modified procedure [1], a quartz tube measuring 10 × 8 mm (o.d. × i.d.) was charged with 1,3,5-triformylphloroglucinol (Tp) (63 mg, 0.3 mmol), 1,4-phenylenediamine (Pa-1) (48 mg, 0.45 mmol) or 2,5-dimethyl-p-phenylenediamine (Pa-2) (61 mg, 0.45 mmol), 1 mL of dioxane, 2 mL of mesitylene, and 0.5 mL of 3 M aqueous acetic acid. The tube was flash frozen at 77 K in liquid N_2 bath, degassed by three freeze-pump-thaw cycles, and flame sealed. The reaction was heated at 120 ºC for 72 h yielding a red precipitate at the bottom of the tube. The powder was isolated by centrifugation and washed with acetone (25 mL×3), and dried at room temperature and evacuated under vacuum at 100 ºC, 12 h to afford a red powder.

COF Tp-TAPT and Tp-TAPB: A quartz tube measuring 10 × 8 mm (o.d. × i.d.) was charged with 1,3,5-triformylphloroglucinol (Tp) (42 mg, 0.2 mmol), 2,4,6-Tris(4-aminophenyl)-1,3,5-triazine (TAPT) (71 mg, 0.2 mmol) or 1,3,5-Tris(4-aminophenyl)benzene (TAPB) (70 mg, 0.2 mmol), 1 mL of dioxane, 2 mL of mesitylene, and 0.5 mL of 3 M aqueous acetic acid. The tube was flash frozen at 77 K in liquid N_2 bath, degassed by three freeze-pump-thaw cycles, and flame sealed. The reaction was heated at 120 ºC for 72 h yielding a yellowish-brown precipitate at the bottom of the tube. The powder was isolated by centrifugation and washed with acetone (25 mL×3), and dried at room temperature and evacuated under vacuum at 100 ºC, 12 h to afford an orange powder.

COF Tp-ABA$_x$-Pa-1 and Tp-ABA$_x$-Pa-2: Following the procedure for COF TpPa-1 and TpPa-2 except a certain amount of 4-aminobenzaldehyde (ABA) were added after Tp (The exact amount to be added can be found in Table S1). The powder was isolated by centrifugation and washed with acetone (25 mL×3), and dried at room temperature and evacuated under vacuum at 100 ºC, 12 h to afford a red powder.

COF Tp-ABA$_x$-TAPT and Tp-ABA$_x$-TAPB: Following the procedure for COF Tp-TAPT and Tp-TAPB except a certain amount of 4-aminobenzaldehyde (ABA) were added after Tp (The exact amount to be added can be found in Table S1). The powder was isolated by centrifugation and washed with acetone (25 mL×2), chloroform (15 mL×2) and hexanes (15 mL×1), and dried at room temperature and evacuated under vacuum at 100 ºC, 12 h to afford an orange or yellow powder.

Table S1. Amounts of monomers used to synthesize COFs.

COF		Tp (mg)	ABA (mg)	Amine (mg)	Product (mg)	Yield (%)
TpPa-1		63.0	0	48.7	97.4	87.2
Tp-ABA$_x$-Pa-1	x=0.2		10.9		104.4	85.2
	x=0.4		21.8		114.8	86.0
	x=0.6		32.7		107.5	74.4
	x=0.8		43.6		118.2	76.1
	x=1		54.5		122.2	73.5
	x=1.5		82.0		130.7	67.5
	x=2		109.0		134.7	61.0
TpPa-2		63.0	0	61.2	105.7	85.1
Tp-ABA$_x$-Pa-2	x=0.25		13.6		117.6	85.3
	x=0.5		27.3		128.4	84.8

	x=0.75		40.9		142.0	86.0
	x=1		54.5		140.4	78.6
	x=1.5		81.8		133.4	64.8
	x=2		109.0		135.5	58.1
Tp-TAPT			0		102.8	91.1
Tp-ABA$_x$-TAPT	x=0.75	42.0	18.2	70.8	110.0	84.0
	x=1.5		36.3		125.3	84.0
	x=2.25		54.5		138.3	82.7
	x=3		72.6		137.5	74.2
	x=4.5		109.0		143.8	64.8
	x=6		145.3		144.3	55.9
Tp-TAPB			0		107.2	95.5
Tp-ABA$_x$-TAPB	x=0.75	42.0	18.2	70.2	119.1	91.3
	x=1.5		36.3		126.8	85.4
	x=2.25		54.5		135.2	81.1
	x=3		72.6		137.1	74.2
	x=4.5		109.0		143.2	64.7
	x=6		145.3		147.3	57.2

Section S3 Powder X-ray diffraction analysis

Pawley refinements were performed using the Reflex module in Materials Studio. All the patterns were refined using the Pseudo-Voigt function, with all FWHM parameters (U, V, W), profile parameters (NA, NB), and line shift allowed to vary. Lattice parameter were also refined.

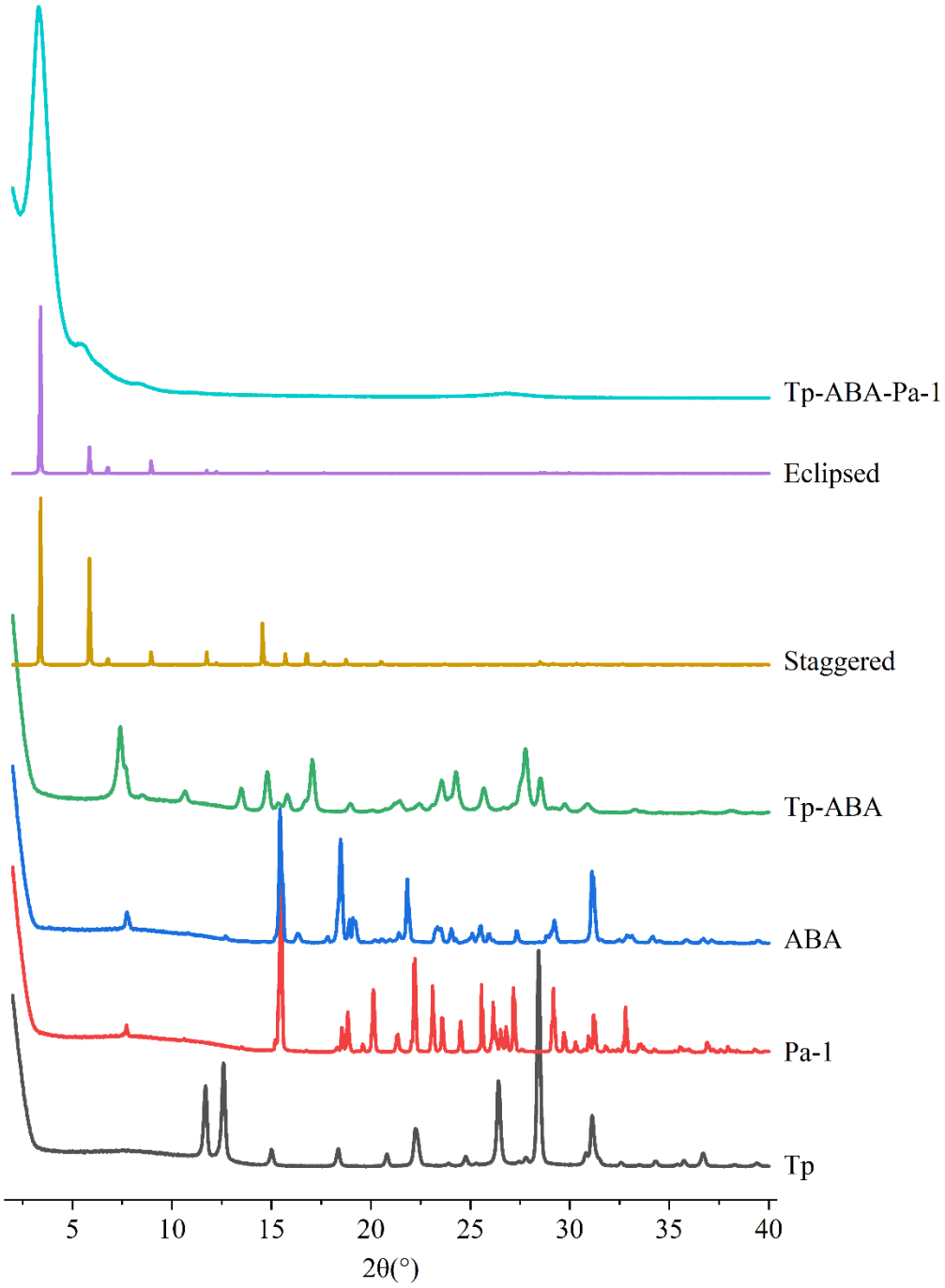

Figure S1. Stacked PXRD spectra of Monomers, product of Tp react with ABA, and simulated PXRD patterns compared with the experimental spectra of Tp-ABA-Pa-1 COF.

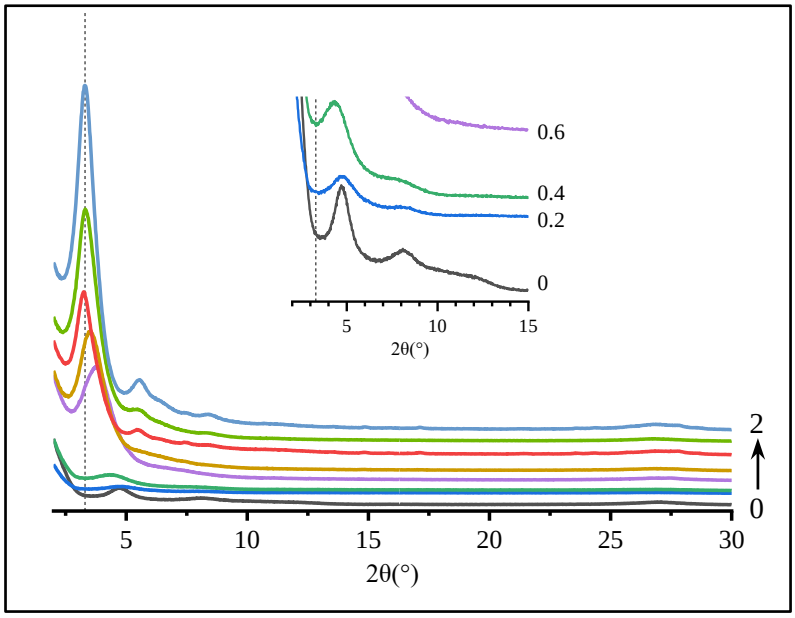

Figure S2. The original PXRD patterns of Tp-ABA$_x$-Pa-1 COFs.

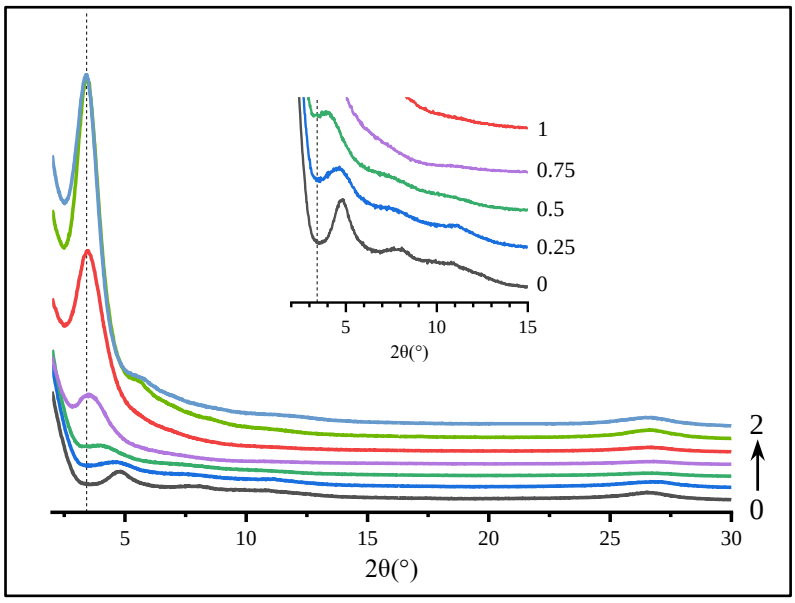

Figure S3. The original PXRD patterns of Tp-ABA$_x$-Pa-2 COFs.

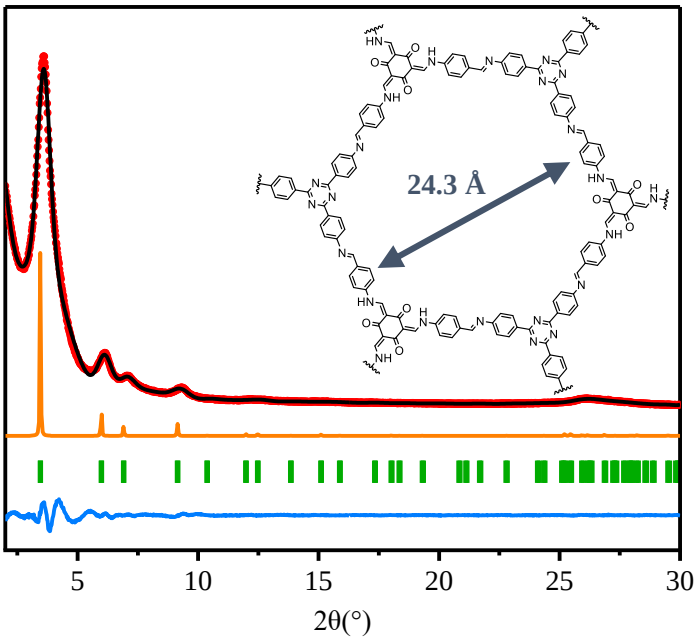

Figure S4. PXRD patterns of Tp-ABA-TAPT COF (red pots: experimentally observed, black: Pawley refinement, blue: their difference, orange: simulated with eclipsed mode, green: Brag position.)

R_p = 3.10%, R_{wp} = 4.27%.

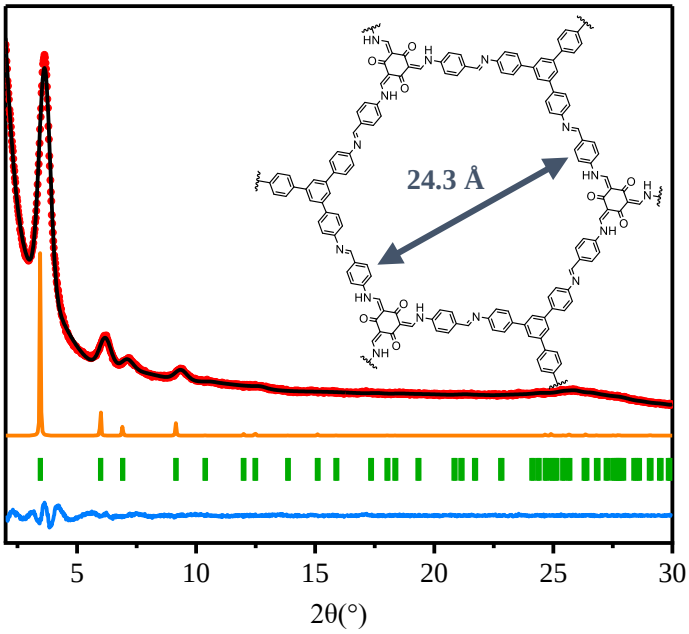

Figure S5. PXRD patterns of Tp-ABA-TAPB COF (red pots: experimentally observed, black: Pawley refinement, blue: their difference, orange: simulated with eclipsed mode, green: Brag position.)

R_p = 2.05, R_{wp} = 2.61%.

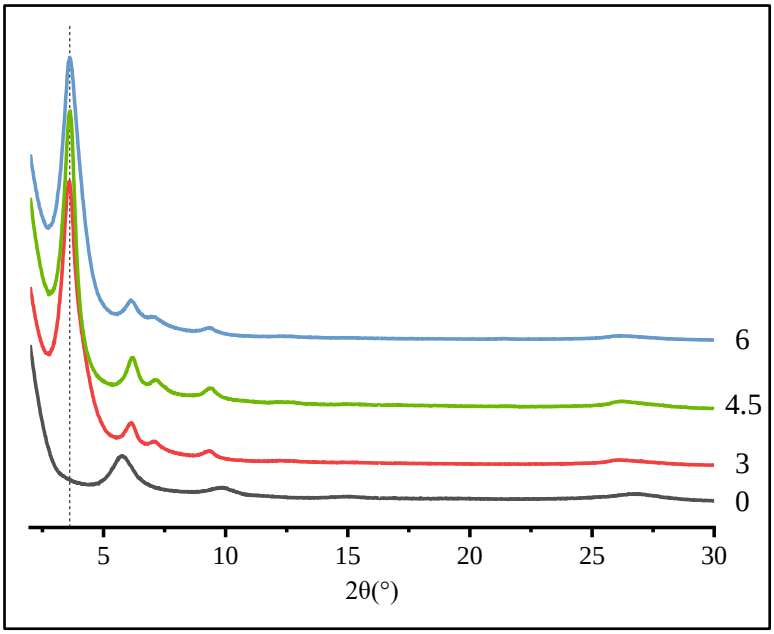

Figure S6. The original PXRD patterns of Tp-ABA$_x$-TAPT COFs.

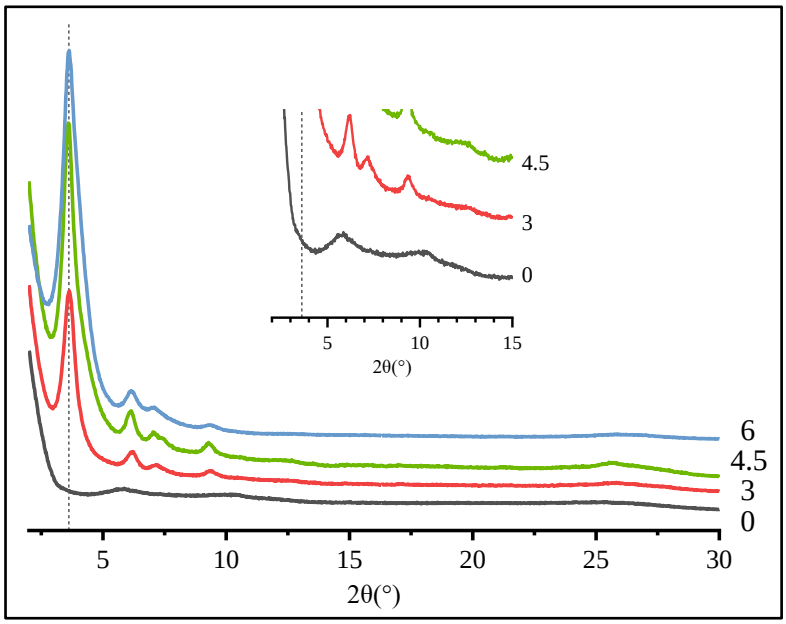

Figure S7. The original PXRD patterns of Tp-ABA$_x$-TAPB COFs.

Section S4 Structure modeling

Structural models of COFs were generated using the Accelrys Materials Studio 7.0 software package. The proposed model was geometry optimized using the Forcite Module (Universal force fields, Ewald summations) to obtain the optimized lattice parameters.

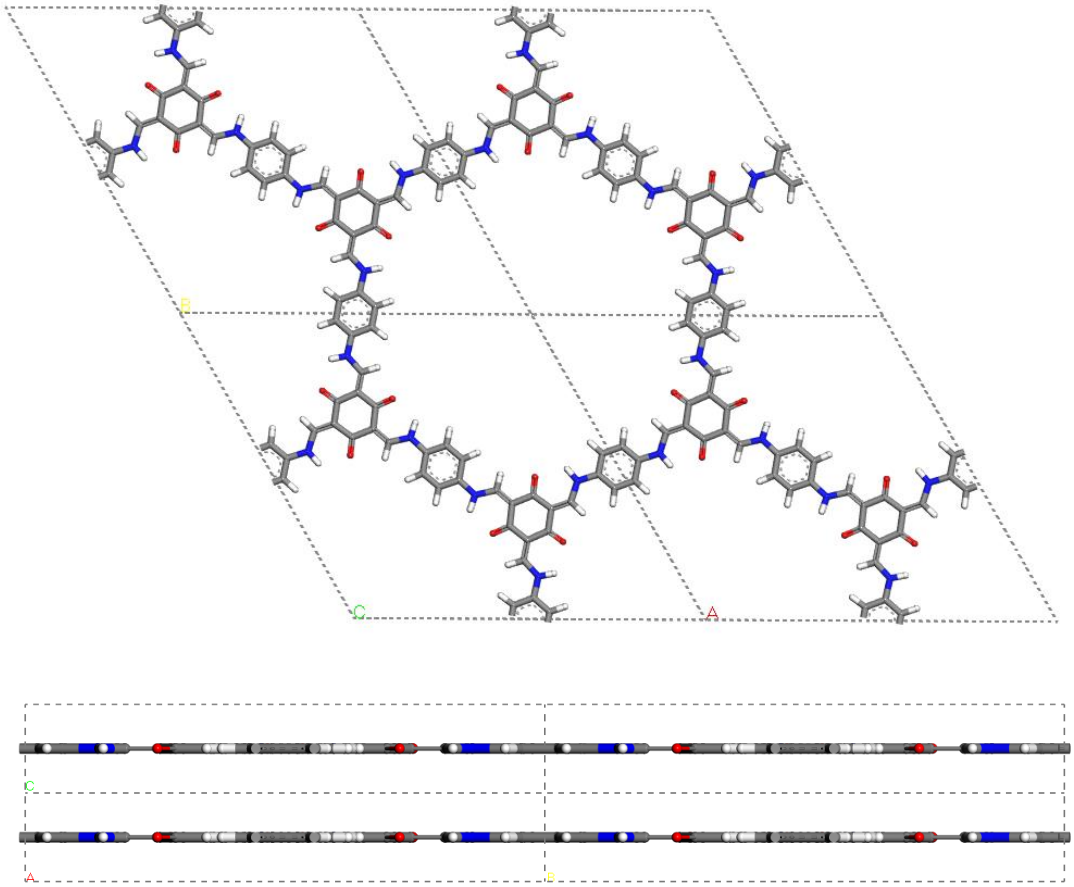

Figure S8. 2×2×2 cells of TpPa-1 COF from Materials Studio.

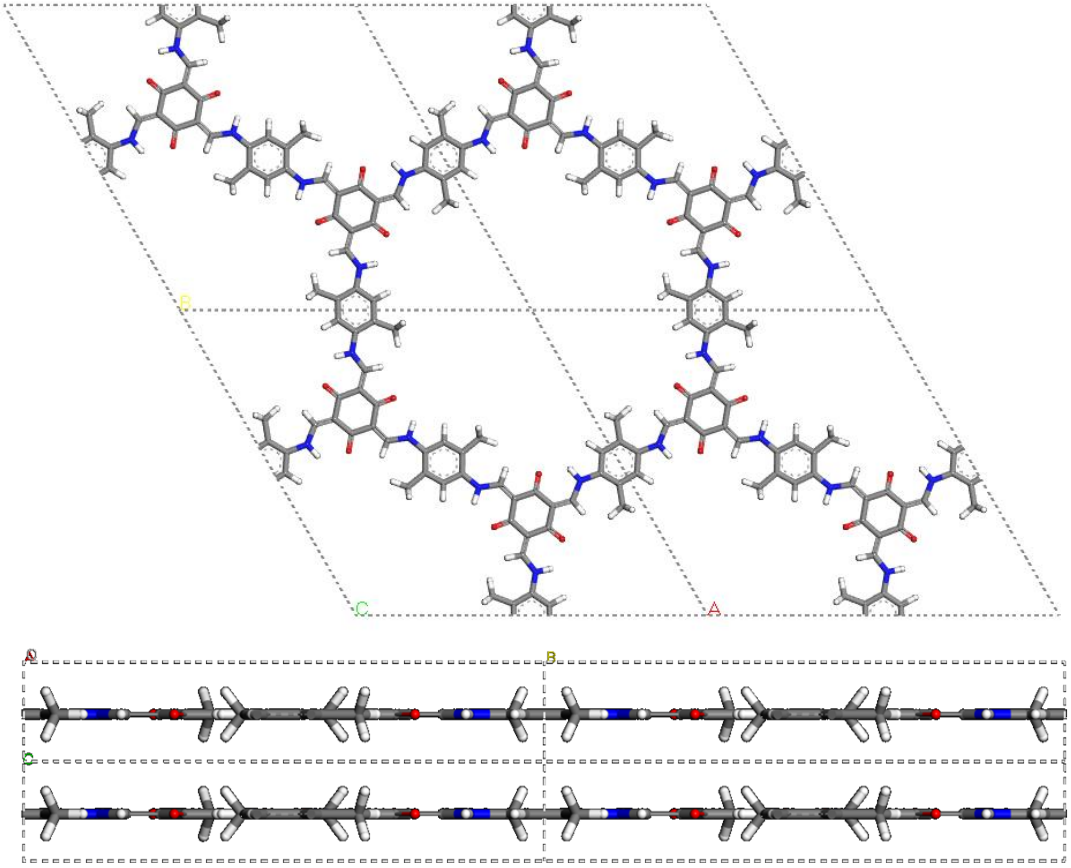

Figure S9. 2×2×2 cells of TpPa-2 COF from Materials Studio.

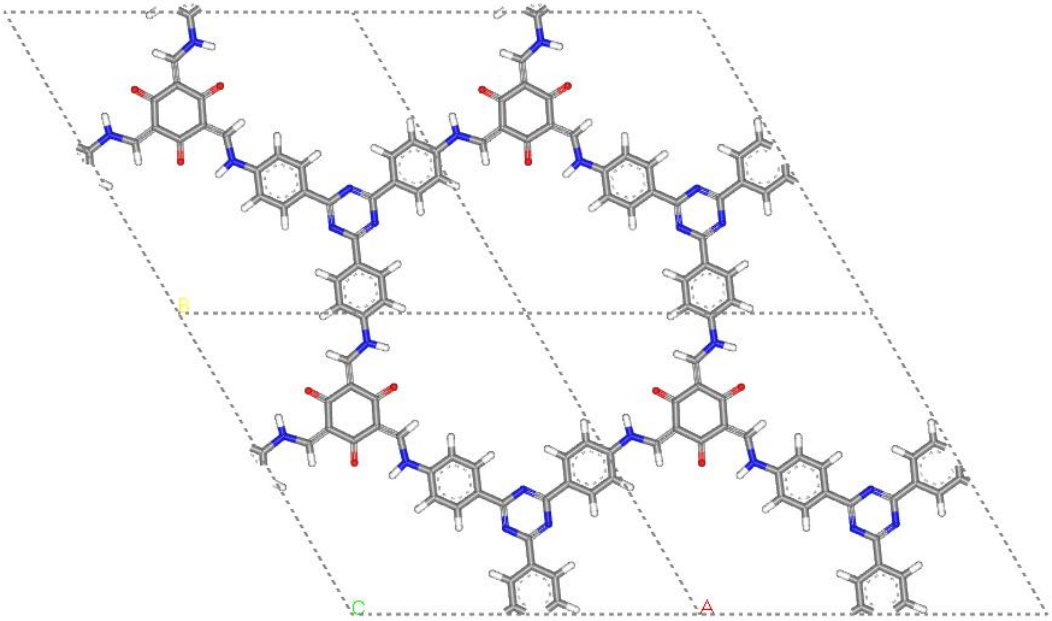

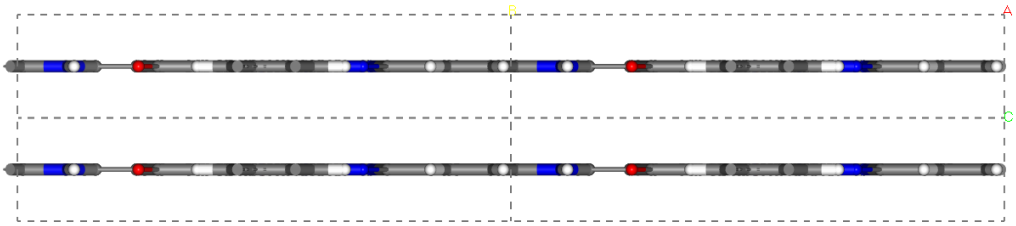

Figure S10. 2×2×2 cells of Tp-TAPT COF from Materials Studio.

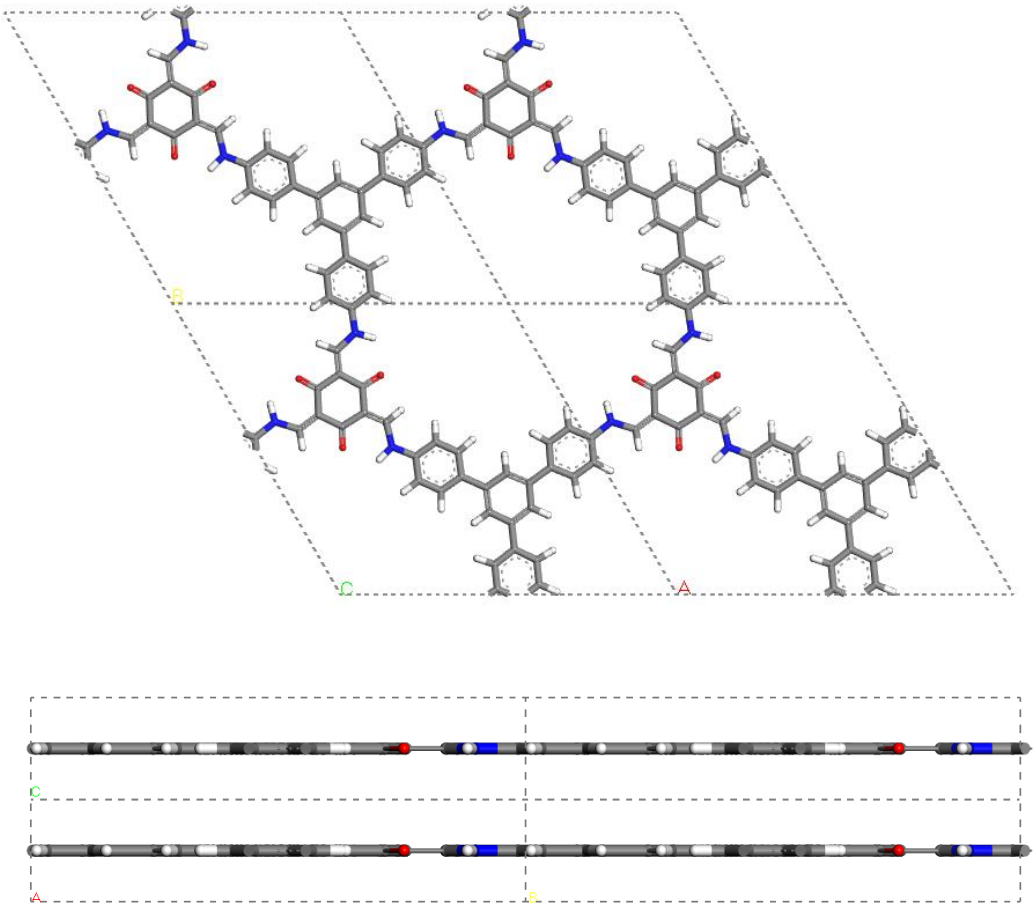

Figure S11. 2×2×2 cells of Tp-TAPB COF from Materials Studio.

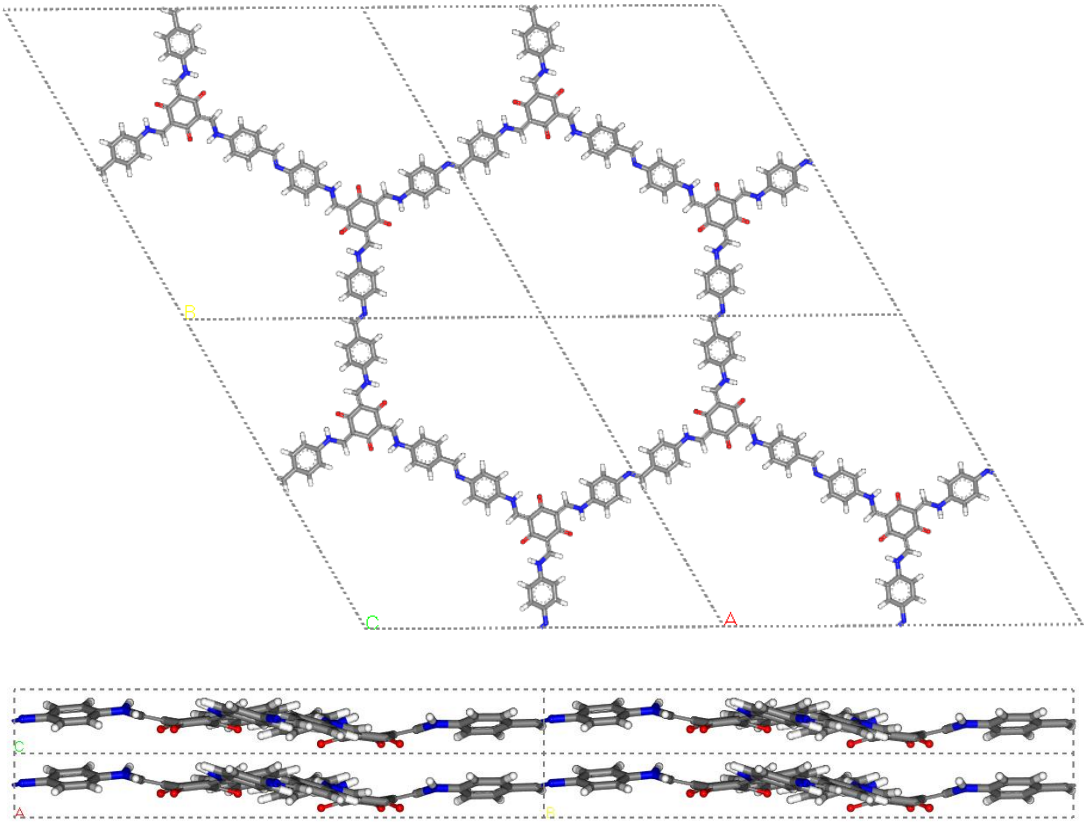

Figure S12. 2×2×2 cells of Tp-ABA-Pa-1 COF from Materials Studio.

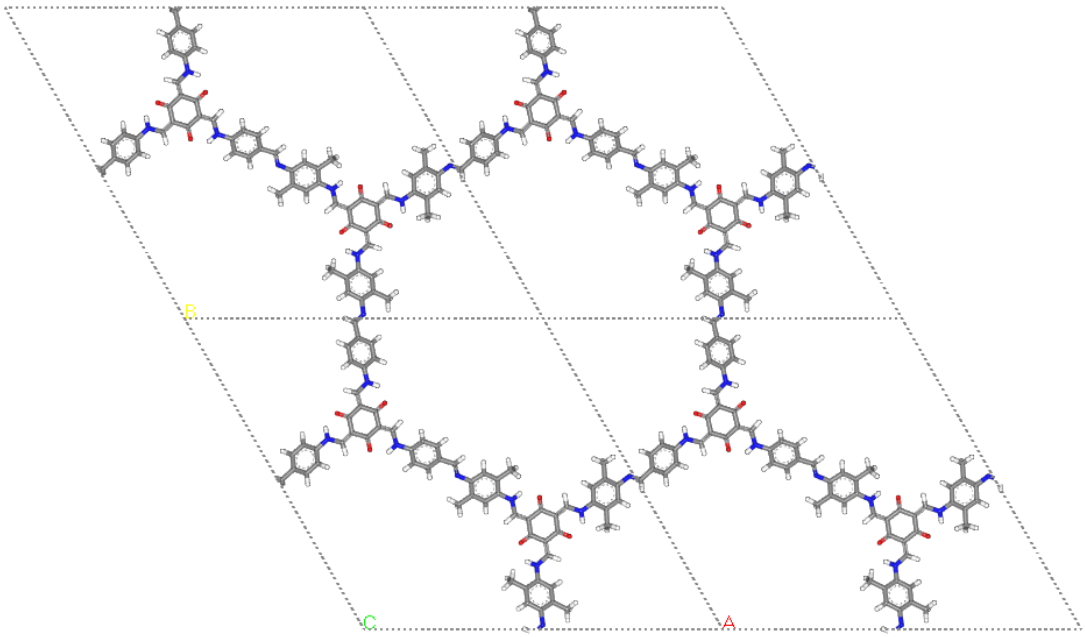

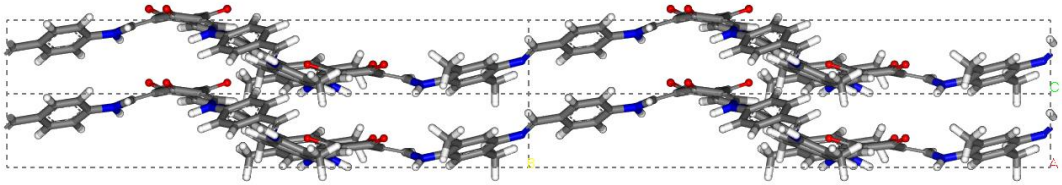

Figure S13. 2×2×2 cells of Tp-ABA-Pa-2 COF from Materials Studio.

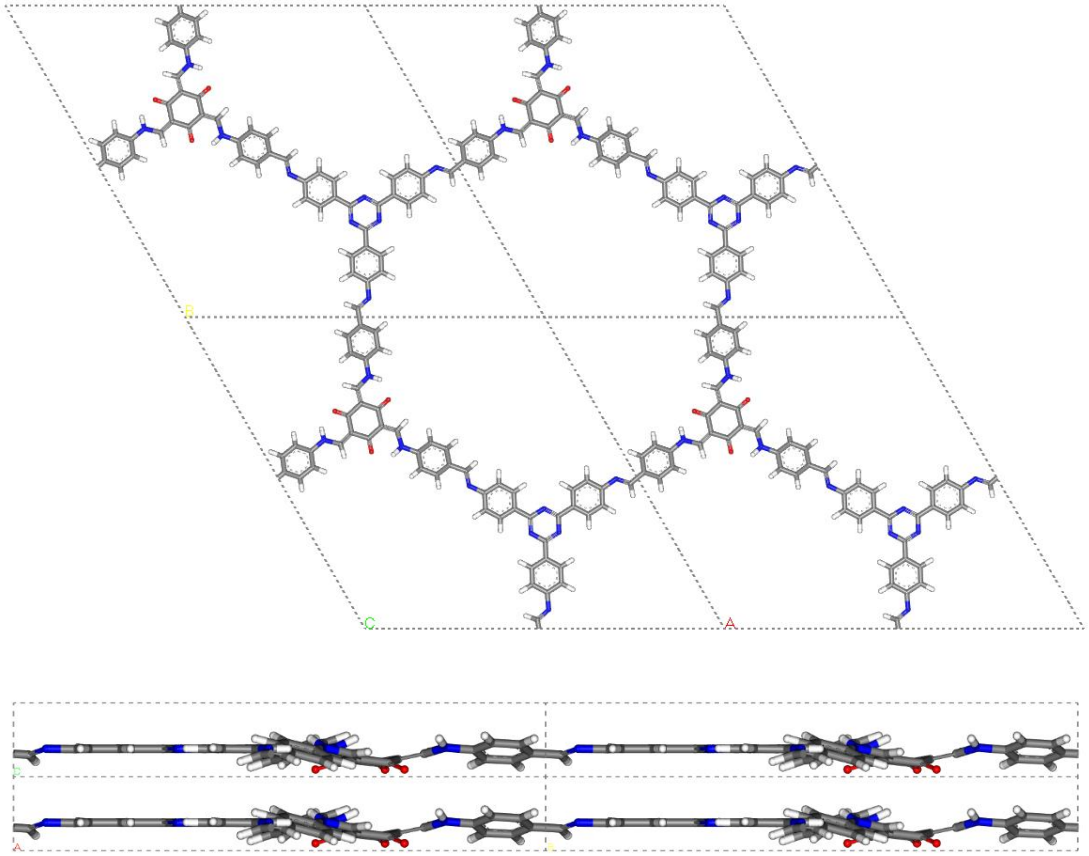

Figure S14. 2×2×2 cells of Tp-ABA-TAPT COF from Materials Studio.

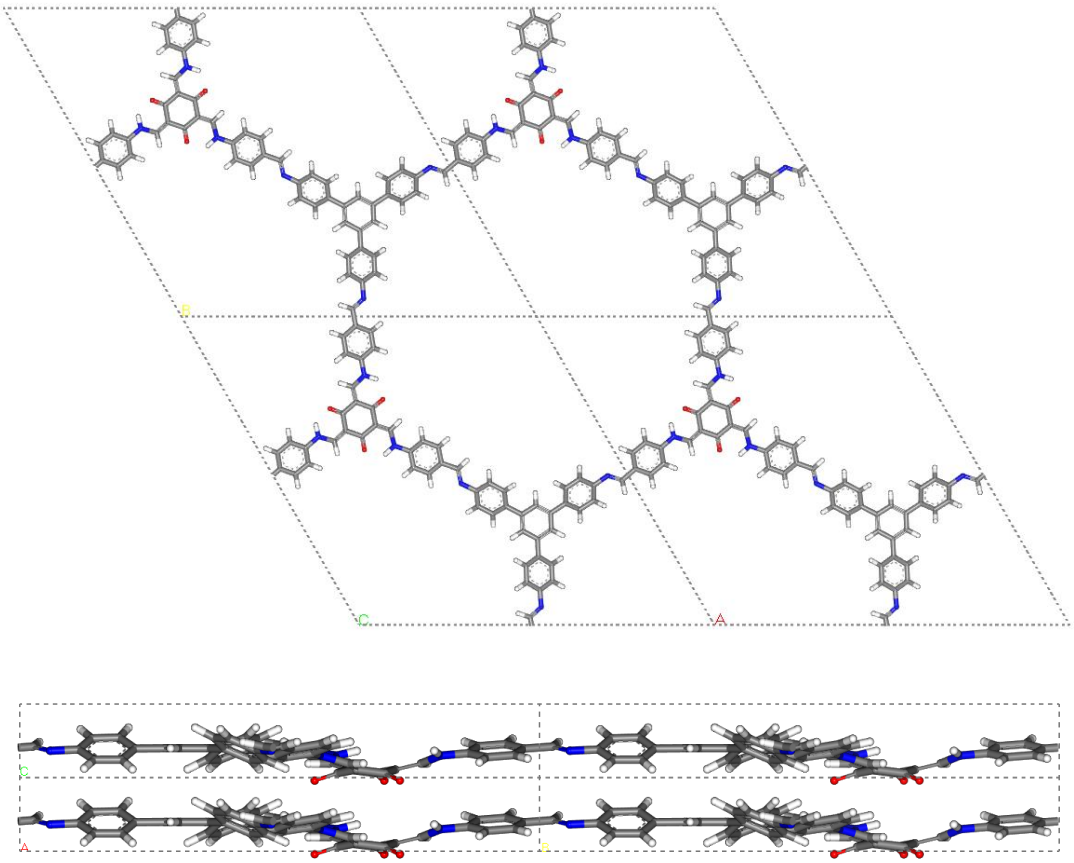

Figure S15. 2×2×2 cells of Tp-ABA-TAPB COF from Materials Studio.

Section S5 N_2 isotherm, BET surface area, and pore width distribution

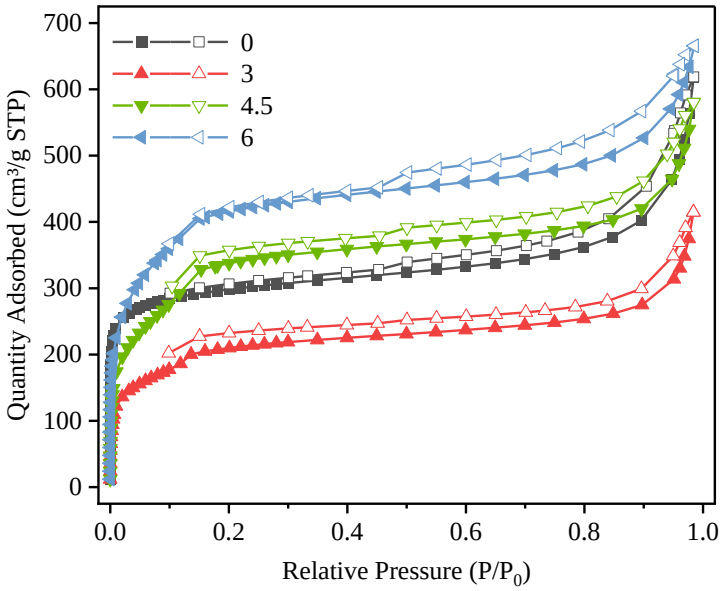

Figure S16. N_2 adsorption (filled symbols) and desorption (empty symbols) isotherms of Tp-ABA$_x$-TAPT COFs.

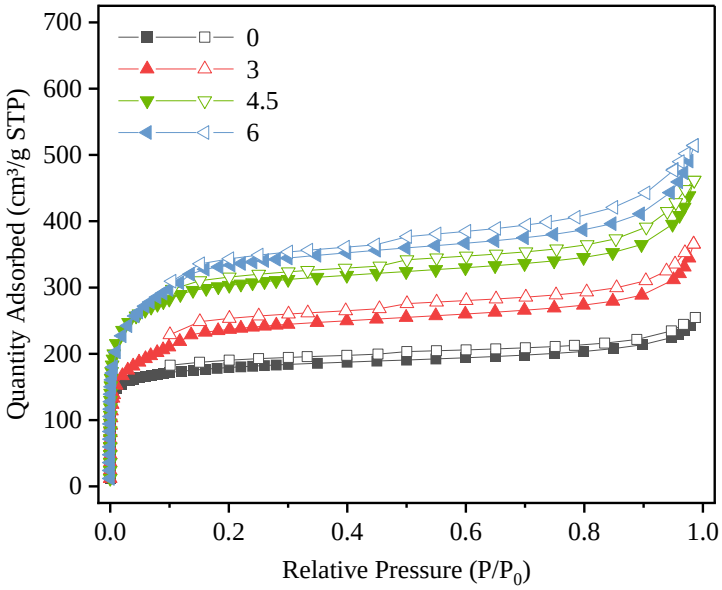

Figure S17. N_2 adsorption (filled symbols) and desorption (empty symbols) isotherms of Tp-ABA$_x$-TAPB COFs.

Table S2. BET surface area values of Tp-ABA series COFs.

Tp-ABA$_x$-Pa-1			Tp-ABA$_x$-Pa-2			Tp-ABA$_x$-TAPT			Tp-ABA$_x$-TAPB	
Mole ratio of ABA/Pa-1	surface area (m^2/g)		Mole ratio of ABA/Pa-2	surface area (m^2/g)		Mole ratio of ABA/TAPT	surface area (m^2/g)		Mole ratio of ABA/TAPB	surface area (m^2/g)
0	592		0	230		0	1126		0	681
0.2	877		0.25	700		3	728		3	857
0.4	993		0.5	838		4.5	1137		4.5	1133
0.6	1138		0.75	989		6	1513		6	1213
0.8	1521		1	1352						
1	1526		1.5	1488						
1.5	1770		2	1297						
2	1846									

Table S3. The observed and predicted BET surface areas of Tp- and Tp-ABA series COFs.

COF	Observed BET	Predicted BET	Observed/ Predicted	COF	Observed BET	Predicted BET	Observed/ Predicted
TpPa-1	592	1622	37%	Tp-ABA-Pa-1	1846	2127	87%
TpPa-2	230	1810	13%	Tp-ABA-Pa-2	1488	1811	82%
Tp-TAPT	1126	1440	78%	Tp-ABA-TAPT	1513	2022	75%
Tp-TAPB	681	1485	46%	Tp-ABA-TAPB	1213	2099	58%

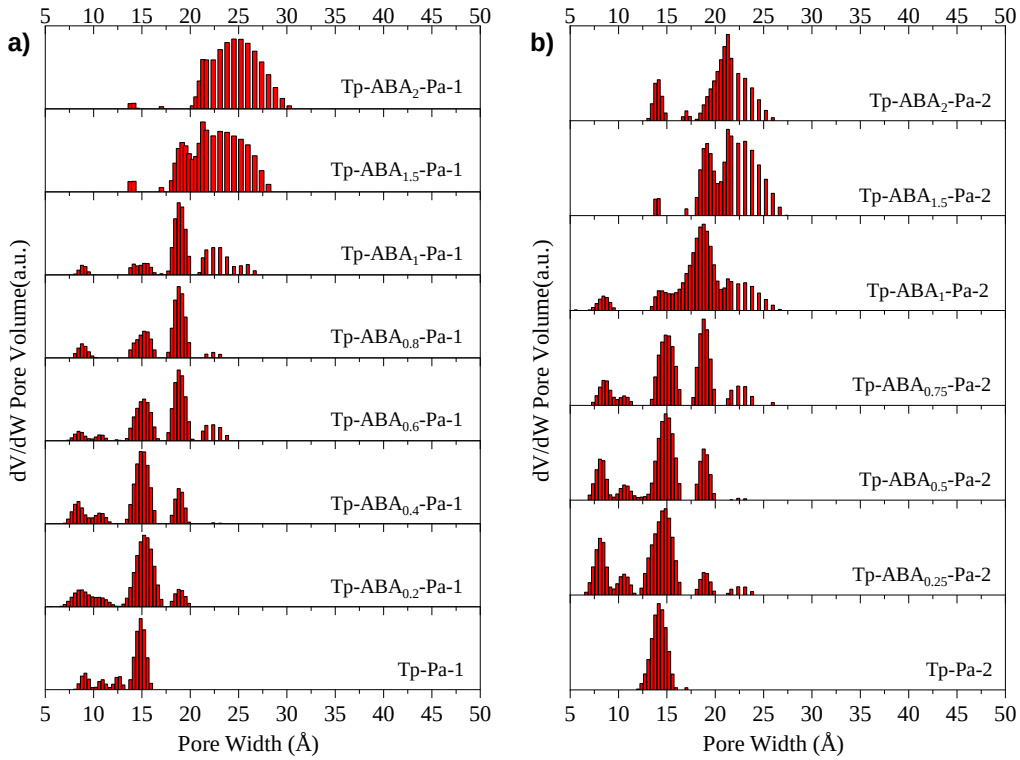

Figure S18. Pore width distributions of (a) Tp-ABA$_x$-Pa-1 COFs and (b) Tp-ABA$_x$-Pa-2 COFs derived from N_2 sorption isotherm measured at 77 K, fitted with DFT model of N_2 on Cylindrical Pores.

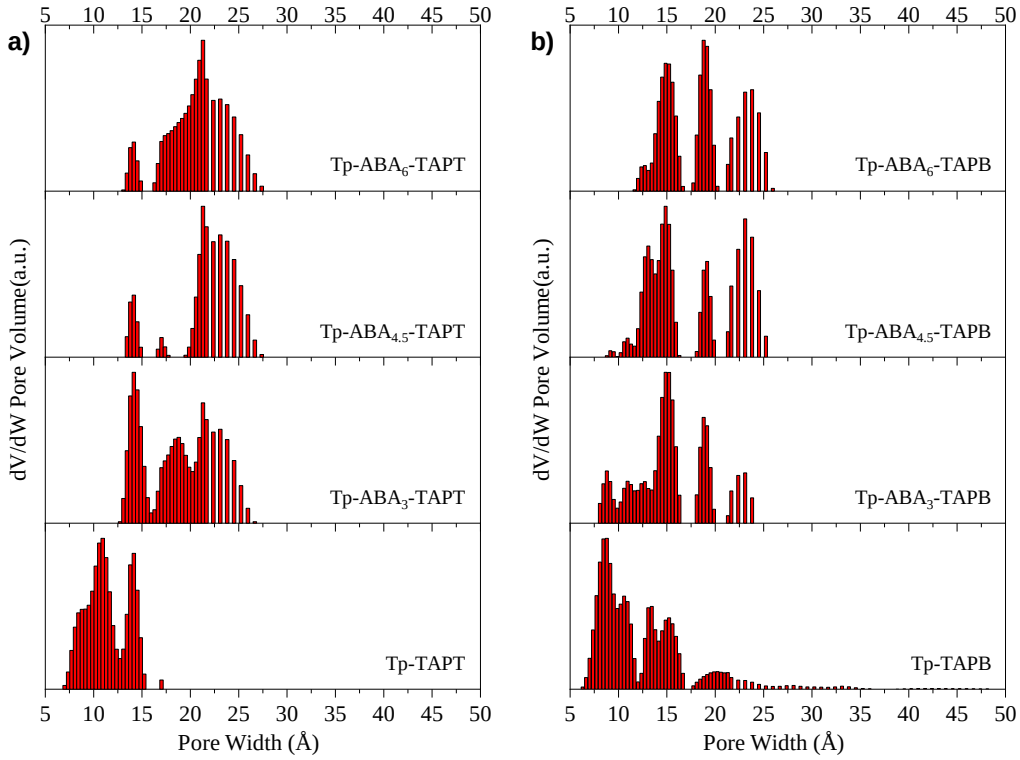

Figure S19. Pore width distributions of (a) Tp-ABA$_x$-TAPT COFs and (b) Tp-ABA$_x$-TAPB COFs derived from N_2 sorption isotherm measured at 77 K, fitted with DFT model of N_2 on Cylindrical Pores.

Section S6 Nuclear magnetic resonance (NMR) spectra

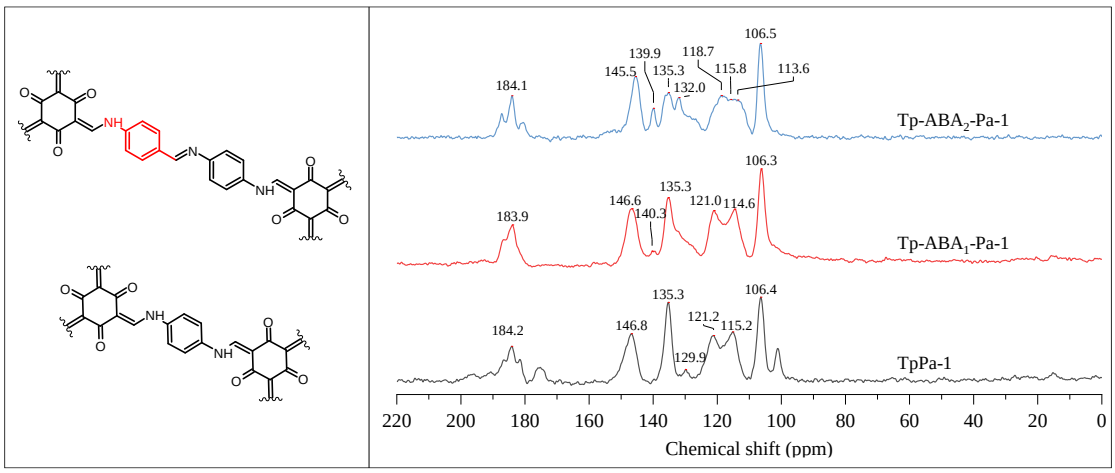

Figure S20. ^{13}C ssNMR spectra of selected Tp-ABA$_x$-Pa-1 COFs.

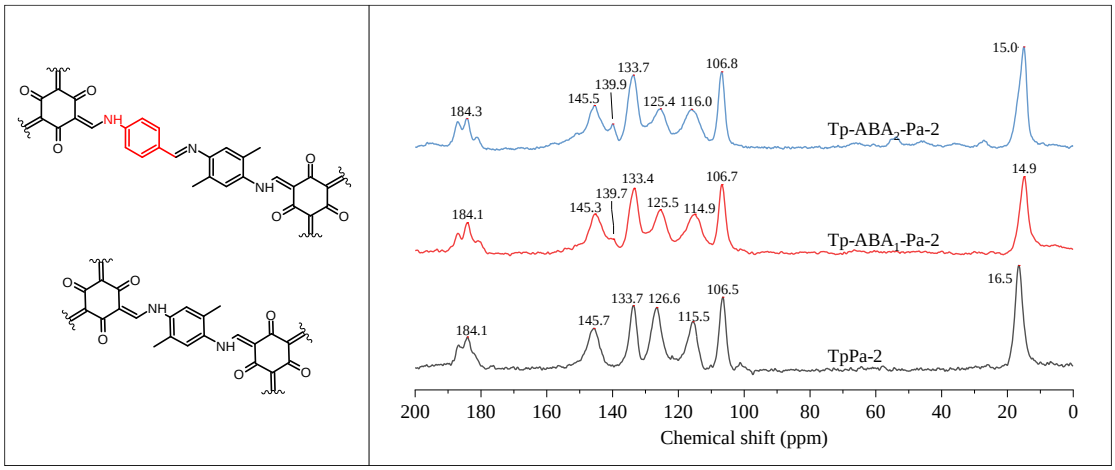

Figure S21. ^{13}C ssNMR spectra of selected Tp-ABA$_x$-Pa-2 COFs.

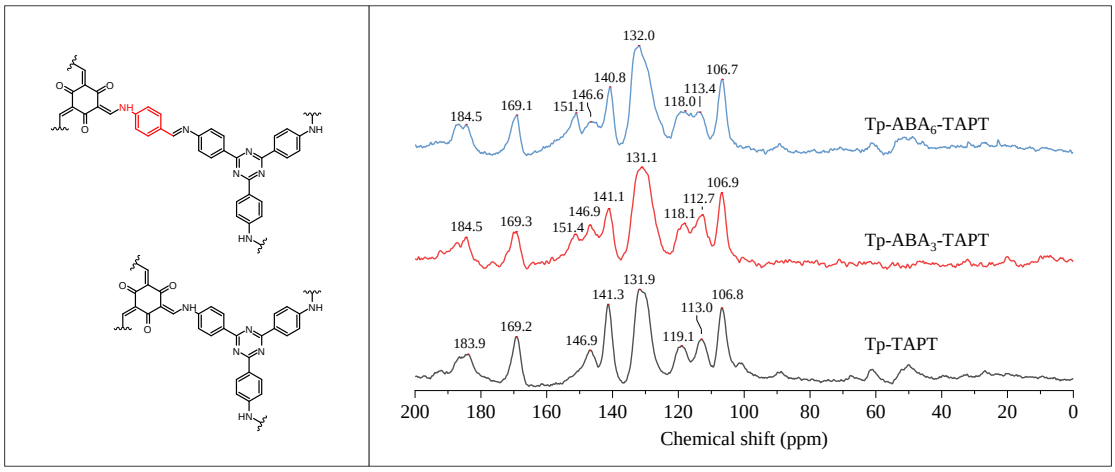

Figure S22. ^{13}C ssNMR spectra of selected Tp-ABA$_x$-TAPT COFs.

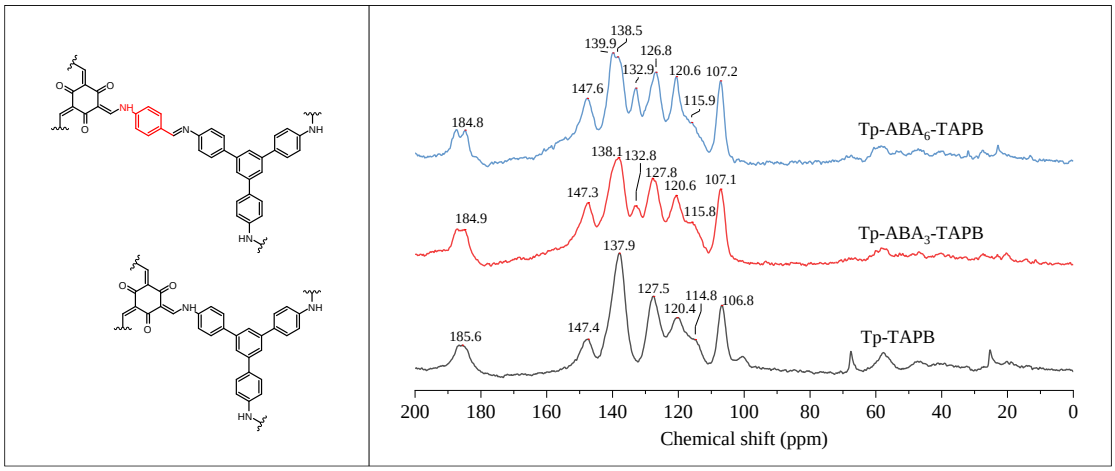

Figure S23. ^{13}C ssNMR spectra of selected Tp-ABA$_x$-TAPB COFs.

Section S7 Fourier-transform infrared (FTIR) spectra

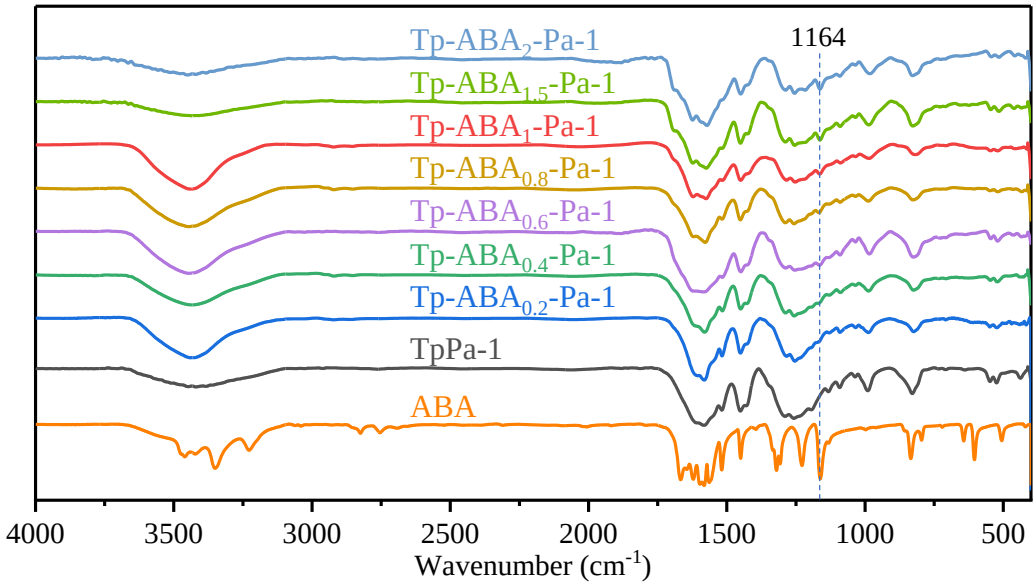

Figure S24. FTIR spectra of ABA and Tp-ABA$_x$-Pa-1 COFs.

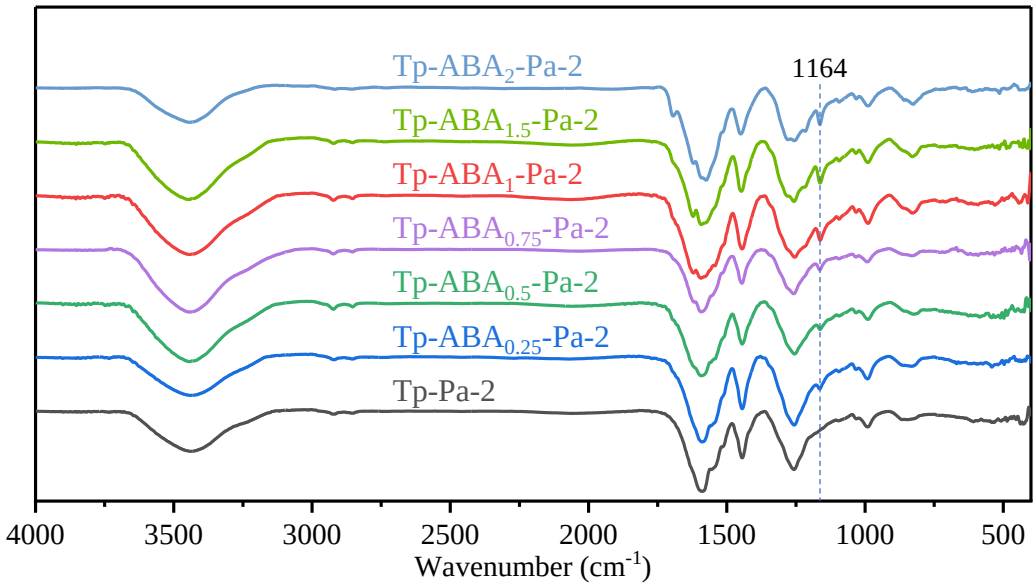

Figure S25. FTIR spectra of Tp-ABA$_x$-Pa-2 COFs.

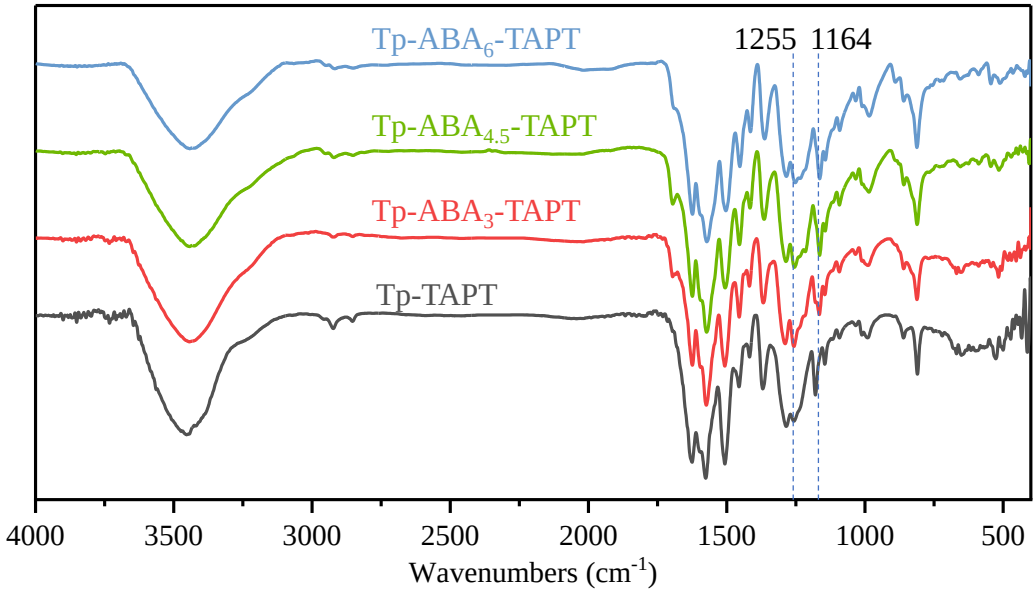

Figure S26. FTIR spectra of Tp-ABA$_x$-TAPT COFs.

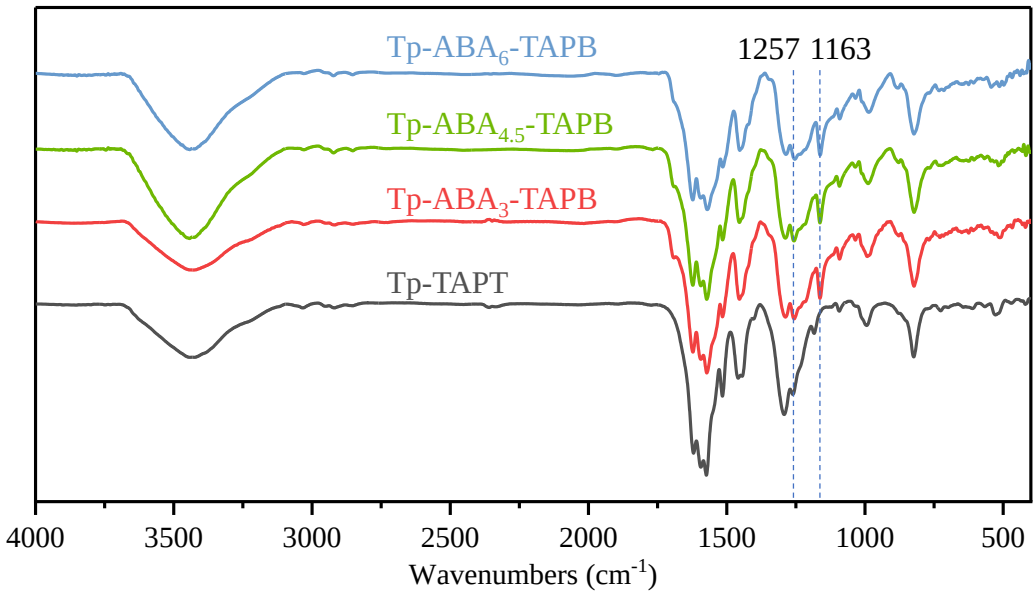

Figure S27. FTIR spectra of Tp-ABA$_x$-TAPB COFs.

Section S8 Thermogravimetric analysis (TGA)

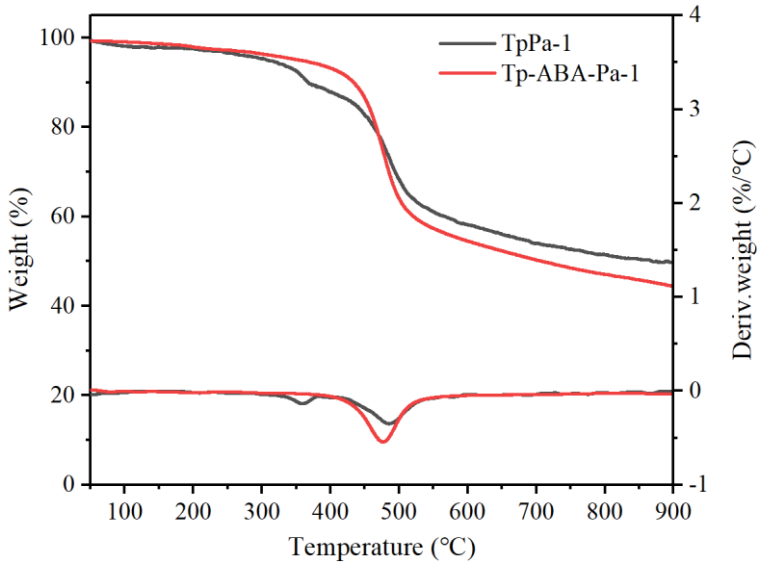

Figure S28. TGA data of TpPa-1 COF compare with Tp-ABA-Pa-1 COF.

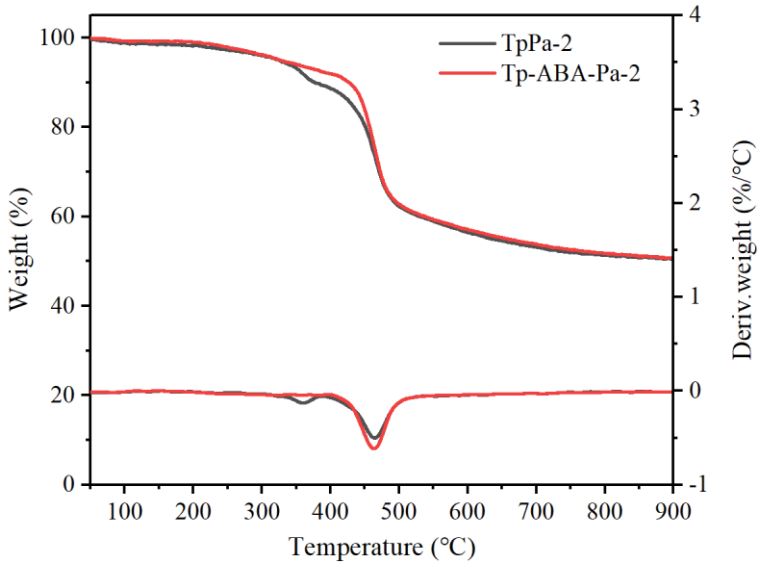

Figure S29. TGA data of TpPa-2 COF compare with Tp-ABA-Pa-2 COF.

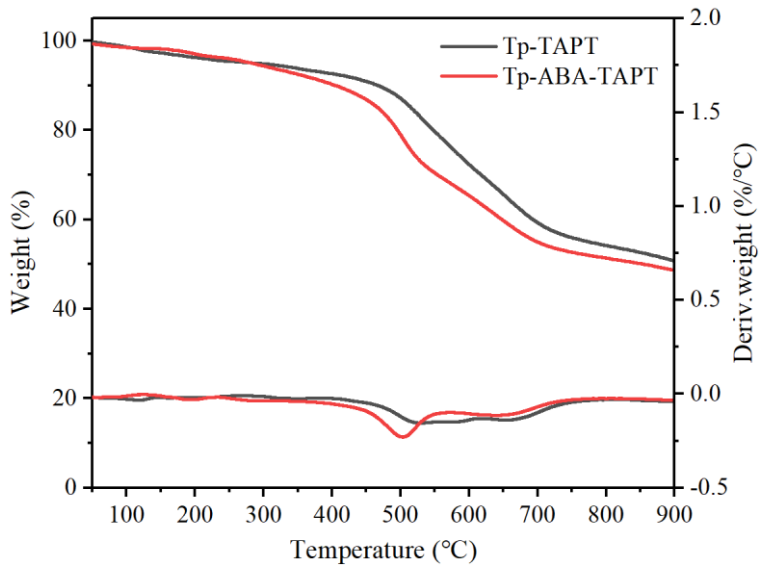

Figure S30. TGA data of Tp-TAPT COF compare with Tp-ABA-TAPT COF.

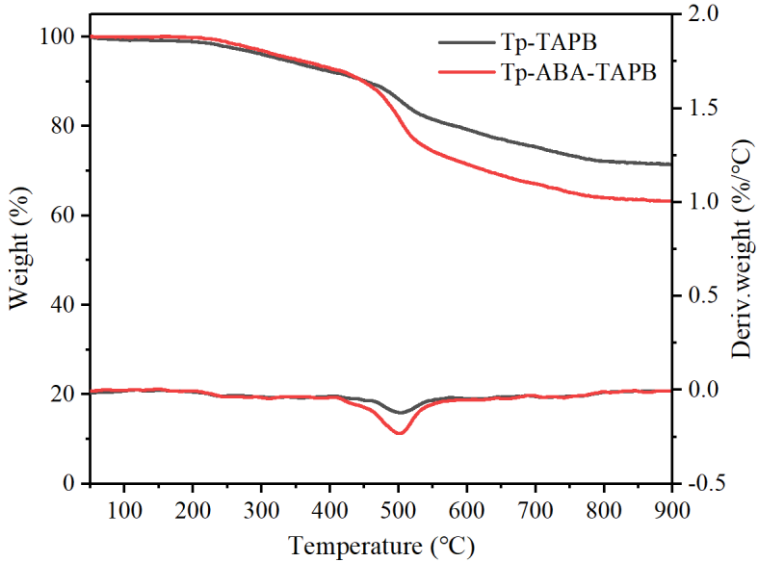

Figure S31. TGA data of Tp-TAPB COF compare with Tp-ABA-TAPB COF.

Section S9 X-ray photoelectron spectroscopy (XPS) analysis

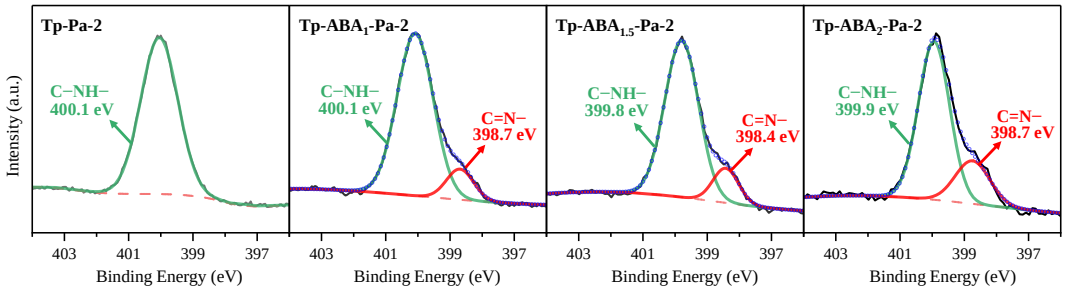

Figure S32. N 1s XPS spectra of selected Tp-ABA$_x$-Pa-2 COFs.

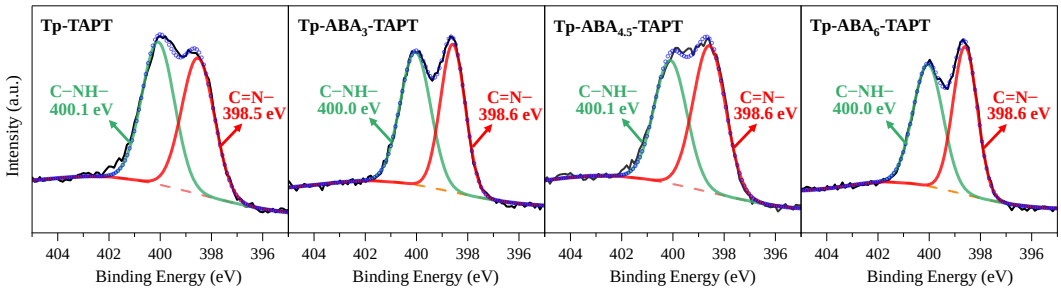

Figure S33. N 1s XPS spectra of Tp-ABA$_x$-TAPT COFs.

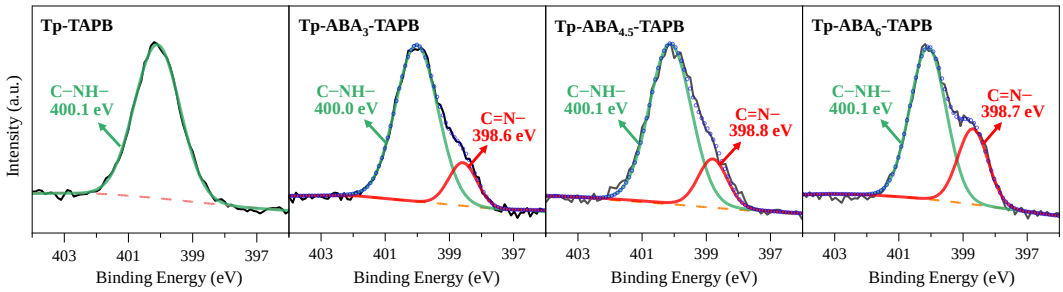

Figure S34. N 1s XPS spectra of Tp-ABA$_x$-TAPB COFs.

Section S10 Conformation of Tp-ABA-Pa-1

As the bifunctional linker ABA can react with both Tp and Pa-1, there are two potential conformations of the connecting arms between each two knots (as shown in the figure below). Therefore, the structural model of Tp-ABA-Pa-1 COF had many possibilities. We found that most potential conformations are not spatially repetitive and thus cannot be represented by a simple model. For Tp-ABA-Pa-1 COF, there are only two simple models that can be repeatedly extended in plane (Model 1 and Model 2), and the other possible conformations need to contain at least four types of cells to extend in plane. We also listed three other possible models for comparison in following figure.

In order to show the different structures of COF more clearly, we replace the connecting arms and knots with the following patterns.

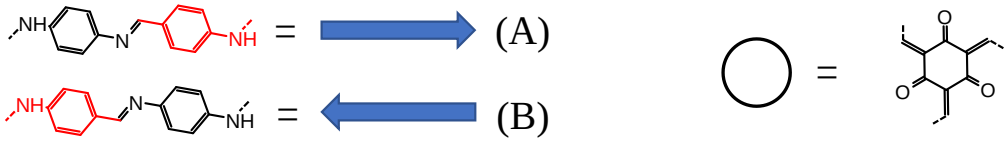

Note that the six letters in parenthesis in the following figure represent the cell type of the six connecting arms clockwise from the left when viewed from the center of the current cell.

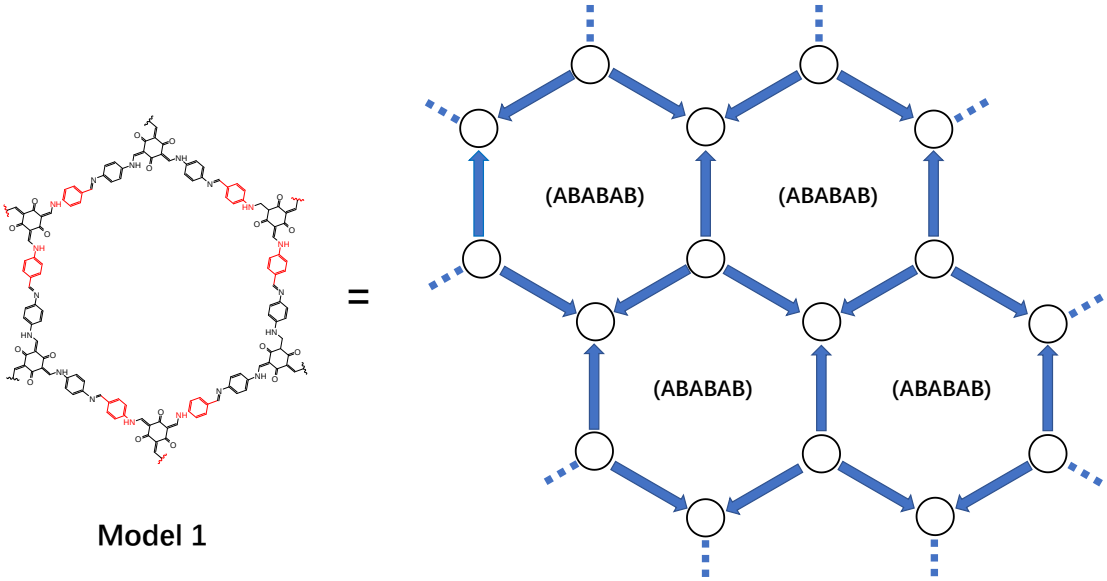

Model 1

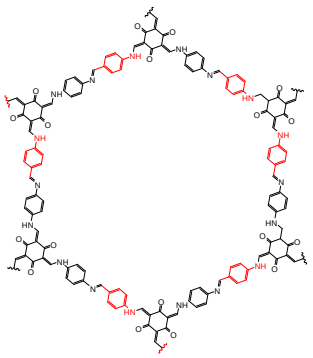

=

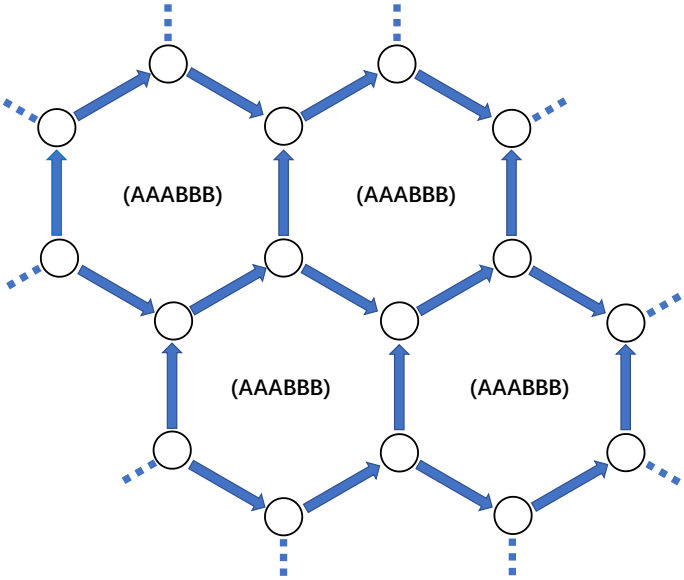

Model 2

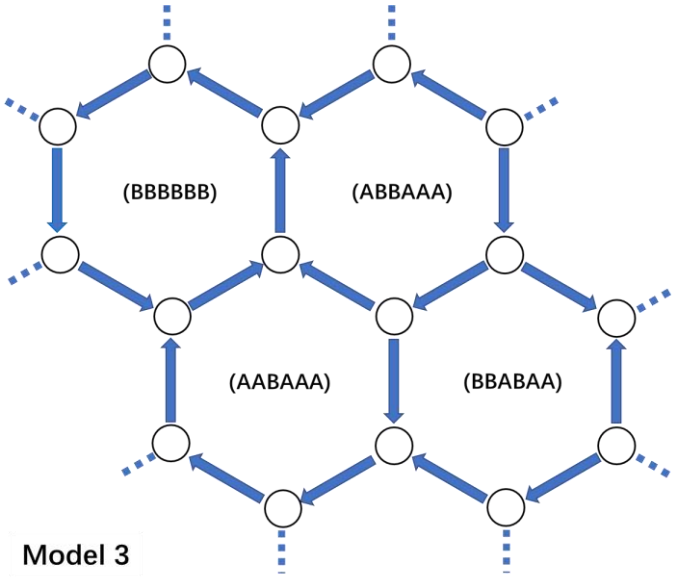

Model 3

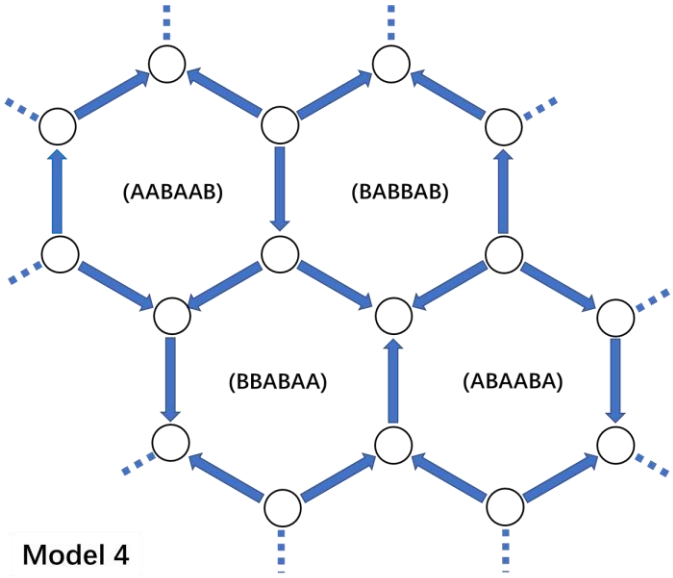

Model 4

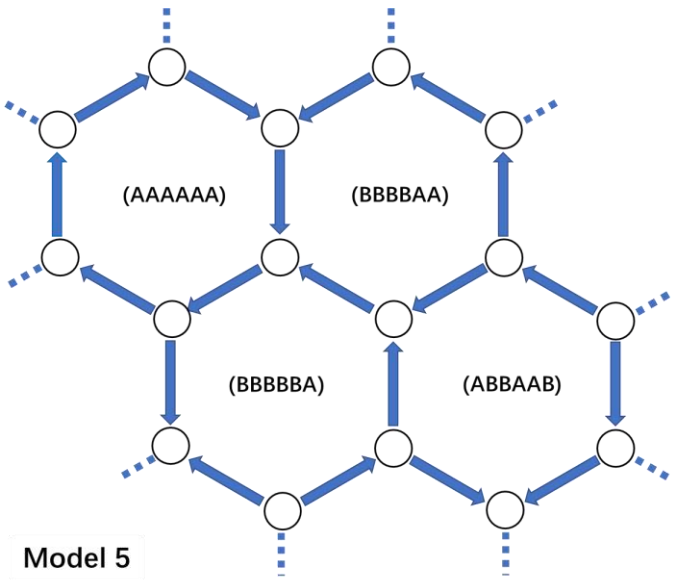

Model	Cell Type				Space Group	Cell parameters			Predicted Total energy	Total energy per cell
	Cell 1	Cell 2	Cell 3	Cell 4		a	b	c	kcal/mol	kcal/mol
1	ABABAB	ABABAB	ABABAB	ABABAB	P3 143	68.05	68.05	3.57	463.41	115.85
2	AAABBB	AAABBB	AAABBB	AAABBB	PM 6	69.32	69.27	3.44	580.12	145.03
3	BBBBBB	ABBAAA	AABAAA	BBABAA	PM 6	69.20	69.26	3.44	580.83	145.21
4	AABAAB	BABBAB	BBABBA	ABAABA	PM 6	69.00	69.36	3.44	575.27	143.82
5	AAAAAA	BBBBAA	BBBBBA	ABBAAB	PM 6	69.22	69.31	3.44	580.74	145.19

The predicted total energy of the other four types of conformations listed in the table is significantly greater than that of Model 1. For these models, the model used in the manuscript (Model 1) that has the lowest energy per cell. Although only five possible conformations are listed, it can be speculated from the table that the predicted total energy of Model 1 is the lowest among all possible conformations: Models 1 and 2 contain only one type of cell, while the other models (including those not listed in the table) contain at least four types of cells. Among these cells, only the cell of model 1 has the lowest energy, so it is only possible that the total energy of model 1 is the lowest. From another point of view, we can also obtain this conclusion: For every knot of Tp-ABA-Pa-1 COF, each knot has three connecting arms in three directions, and only when the types of connecting arms in these three directions are the same, the force on the knot is uniform. It can also be seen from the above structural diagram that only each knot of Model 1 has the most uniform stress.

Since Model 1 has the lowest total energy, that is to say, except the Model 1, all the other models are more thermodynamically unstable, so the products should tend to form the conformation with the lowest energy. It is worth noting that this conformation (Model 1) has the best symmetry among all possible conformations.

Section S11 Atomic coordinates of COFs

Tp-ABA-Pa-1, Pawley refined			*P3* (143)	
$a = b = 30.1271$ Å; $c = 3.1283$ Å				
$\alpha = \beta = 90°$; $\gamma = 120°$				
Atom Name	Atom	x	y	z
C1	C	0.64904	0.28359	0.51309
C2	C	0.51747	0.53212	0.47595
H3	H	0.55288	0.55642	0.42396
C4	C	0.42225	0.5803	0.4561
C5	C	0.40808	0.53532	0.56047
C6	C	0.43862	0.5192	0.56356
C7	C	0.48427	0.54795	0.46448
C8	C	0.49854	0.59277	0.35697
C9	C	0.46786	0.60875	0.34875
C10	C	0.29922	0.68096	0.24388
N11	N	0.38957	0.5955	0.46036
O12	O	0.42056	0.72786	0.14879
C13	C	0.39995	0.64099	0.3715
H14	H	0.4266	0.48445	0.64874
H15	H	0.5335	0.6154	0.27584
H16	H	0.48033	0.64319	0.25576
H17	H	0.43478	0.66804	0.39506
H18	H	0.48735	0.86053	0.64218
C19	C	0.28429	0.63205	0.29055
C20	C	0.61756	0.30169	0.46836
C21	C	0.53387	0.47092	0.56411
C22	C	0.57938	0.49699	0.67957
C23	C	0.60647	0.47701	0.71286
C24	C	0.5889	0.4308	0.63138
C25	C	0.54331	0.40489	0.51432
C26	C	0.51608	0.42479	0.48669
N27	N	0.61813	0.41167	0.67022
C28	C	0.60467	0.36521	0.58754
O29	O	0.57813	0.27654	0.37651
H30	H	0.59383	0.53239	0.75391
H31	H	0.52822	0.36945	0.44195
H32	H	0.48103	0.40429	0.39886
H33	H	0.5691	0.33999	0.60839
H34	H	0.50236	0.14367	0.80525
N35	N	0.5044	0.48966	0.53617
H36	H	0.35743	0.57273	0.56607
H37	H	0.65001	0.43242	0.79023

Tp-ABA-Pa-2, Pawley refined			*P3* (143)	
$a = b = 30.5675$ Å; $c = 3.7218$ Å				
$\alpha = \beta = 90°$; $\gamma = 120°$				
Atom Name	Atom	x	y	z
C1	C	0.64733	0.2825	0.26874
C2	C	0.5188	0.5317	0.62377
H3	H	0.55282	0.55222	0.73716
C4	C	0.42114	0.57814	0.77745
C5	C	0.40738	0.5354	0.61525
C6	C	0.43874	0.51983	0.56688
C7	C	0.4847	0.54679	0.68086
C8	C	0.49839	0.58909	0.84917
C9	C	0.46693	0.60456	0.89965
C10	C	0.29923	0.68191	1.05598
N11	N	0.38781	0.59311	0.81932
O12	O	0.42213	0.7278	1.1495
C13	C	0.39962	0.63929	0.91847
H14	H	0.42708	0.48695	0.43703
H15	H	0.53348	0.61014	0.94369
H16	H	0.47866	0.63675	1.0389
H17	H	0.43523	0.66641	0.89272
H18	H	0.48576	0.85803	0.52174
C19	C	0.28338	0.63208	1.00864
C20	C	0.61648	0.3023	0.30986
C21	C	0.53705	0.47556	0.35995
C22	C	0.58534	0.50142	0.40085
C23	C	0.61327	0.48238	0.31822
C24	C	0.59278	0.43658	0.19247
C25	C	0.54487	0.41155	0.13709
C26	C	0.51693	0.43045	0.22054
N27	N	0.62071	0.41589	0.12108
C28	C	0.60574	0.36857	0.20705
O29	O	0.57622	0.27763	0.39657
H30	H	0.6018	0.53668	0.49314
H31	H	0.52895	0.37724	0.02399
C32	C	0.46572	0.40137	0.15709
H33	H	0.56904	0.34428	0.21259
C34	C	0.48905	0.15372	0.37275
N35	N	0.50778	0.4944	0.44449
H36	H	0.35431	0.5704	0.73235
H37	H	0.6532	0.43646	0.0086
H38	H	0.45216	0.36744	0.29073
H39	H	0.45905	0.39511	-0.1296

H40	H	0.44605	0.41775	0.25505
H41	H	0.45579	0.13035	0.50654
H42	H	0.4811	0.16384	0.11468
H43	H	0.50828	0.18514	0.53735

Tp-ABA-TAPT, Pawley refined			*P3* (143)	
$a = b = 29.5382$ Å; $c = 3.5322$ Å				
$\alpha = \beta = 90°$; $\gamma = 120°$				
Atom Name	Atom	x	y	z
C1	C	0.64226	0.28103	1.37824
C2	C	0.53417	0.50596	1.298
C3	C	0.43042	0.56508	0.36435
C4	C	0.41359	0.51371	0.45891
C5	C	0.44688	0.49405	0.43618
C6	C	0.49802	0.52559	0.31977
C7	C	0.51493	0.5768	0.22222
C8	C	0.48149	0.59636	0.2411
C9	C	0.29548	0.68384	0.19053
C10	C	1.27759	1.62825	0.23567
N11	N	1.61476	1.30565	0.37821
C12	C	1.55053	1.4347	0.37523
C13	C	1.60455	1.46323	0.37981
C14	C	1.63312	1.43819	0.37993
C15	C	1.60845	1.38427	0.37823
C16	C	1.5545	1.35599	0.37854
C17	C	1.52599	1.38107	0.37866
H18	H	1.67461	1.46119	0.38345
H19	H	1.53418	1.31443	0.37912
H20	H	1.48447	1.35859	0.37956
N21	N	1.51921	1.45837	0.37925
H22	H	1.62506	1.50467	0.3899
C23	C	1.40737	1.63561	0.31115
N24	N	1.39476	1.58375	0.39425
O25	O	1.30205	1.56743	0.09782
H26	H	1.44706	1.6656	0.33312
H27	H	1.35891	1.55876	0.51232
H28	H	0.57305	0.53186	1.2051
H29	H	0.37447	0.48876	0.5525
H30	H	0.43267	0.45433	0.51311
H31	H	0.55405	0.60167	0.12787
H32	H	0.49608	0.6357	0.15531

Tp-ABA-TAPB, Pawley refined			*P3* (143)	
$a = b = 29.5272$ Å; $c = 3.6081$ Å				
$\alpha = \beta = 90°$; $\gamma = 120°$				
Atom Name	Atom	x	y	z
C1	C	0.64184	0.27904	1.39844
C2	C	0.53097	0.50603	1.42229
C3	C	0.42582	0.56271	0.33184
C4	C	0.40861	0.51049	0.2778
C5	C	0.44246	0.49166	0.30664
C6	C	0.4943	0.52483	0.39376
C7	C	0.51139	0.57689	0.45501
C8	C	0.47751	0.59572	0.42613
C9	C	0.29718	0.68575	0.0606
C10	C	1.27735	1.62996	0.10892
C11	C	1.61325	1.30434	0.39874
C12	C	1.54753	1.43452	0.3814
C13	C	1.59723	1.45915	0.5333
C14	C	1.62579	1.43422	0.54347
C15	C	1.60606	1.38446	0.39542
C16	C	1.55614	1.36024	0.24423
C17	C	1.52718	1.38473	0.24335
H18	H	1.66277	1.45379	0.67891
H19	H	1.53953	1.32292	0.11469
H20	H	1.48905	1.3653	0.1241
N21	N	1.51616	1.45802	0.36499
H22	H	1.61383	1.49684	0.65609
C23	C	1.40417	1.63212	0.19141
N24	N	1.3898	1.58062	0.29957
O25	O	1.29875	1.56738	-0.03965
H26	H	1.4444	1.66076	0.1919
H27	H	1.35176	1.5542	0.36295
H28	H	0.57057	0.53344	1.48333
H29	H	0.36887	0.48437	0.20831
H30	H	0.42806	0.45124	0.25911
H31	H	0.55101	0.60303	0.52798
H32	H	0.49185	0.63574	0.48661
H33	H	1.57202	1.28197	0.39842

Section S12 References

[1] Kandambeth, S.; Mallick, A.; Lukose, B.; Mane, M. V.; Heine, T.; Banerjee, R. Construction of Crystalline 2D Covalent Organic Frame-works with Remarkable Chemical (Acid/Base) Stability via a Combined Reversible and Irreversible Route. *J. Am. Chem. Soc.* 2012, *134*, 19524-19527.